A deep XMM-Newton observation of the X-Persei-like binary system CXOU J225355.1+624336

N. La Palombara
(IASF Milano)
L. Sidoli, P. Esposito, G. L. Israel, G. A. Rodriguez-Castillo

IASF

CNOC XII
Cefalù
28/09/2022

INAF

The BeXB pulsar CXOU J225355.1+624336

- Discovered by *ROSAT* and included in both the RASS FSC (Voges et al. 2000; 1RXS J225352.8+624354) and the WGA Catalogue (White, Giommi & Angelini 1994; 1WGA J2253.9+6243)
- X-ray counterpart of the INTEGRAL source IGR J22534+6243 (Krivonos et al. 2012)
- 47-s pulsation discovered and reported independently by Halpern (2012) and (within the CATS@BAR project) by Israel & Rodriguez (2012)
- Position consistent with that of the infrared source 2MASS J22535512+6243368 (Halpern 2012; Landi et al. 2012)
- Observed with *Swift* in 2006, *Chandra* in 2009, and *NOT* in 2012 (Esposito et al. 2013)

$\Downarrow$

- Classification of the optical counterpart as a B0-1III-Ve star @ $d \sim$ 4-5 kpc
- $P_{\rm s,ROSAT} = 46.406(5)$ s, $P_{\rm s,Swift} = 46.6145(5)$ s, $P_{\rm s,Chandra} = 46.670(4)$ s $\Rightarrow \dot{P}_{\rm s} \approx 5.3 \times 10^{-10}$ s s^{-1}
- $f_{\rm X} \sim (2\text{-}4) \times 10^{-12}$ erg cm^{-2} s^{-1} $\Rightarrow L_{\rm X} \sim$ a few 10^{34} erg s^{-1}

$\Downarrow$

candidate member of the class of persistent, X-Per-like BeXBs

The BeXB pulsar CXOU J225355.1+624336

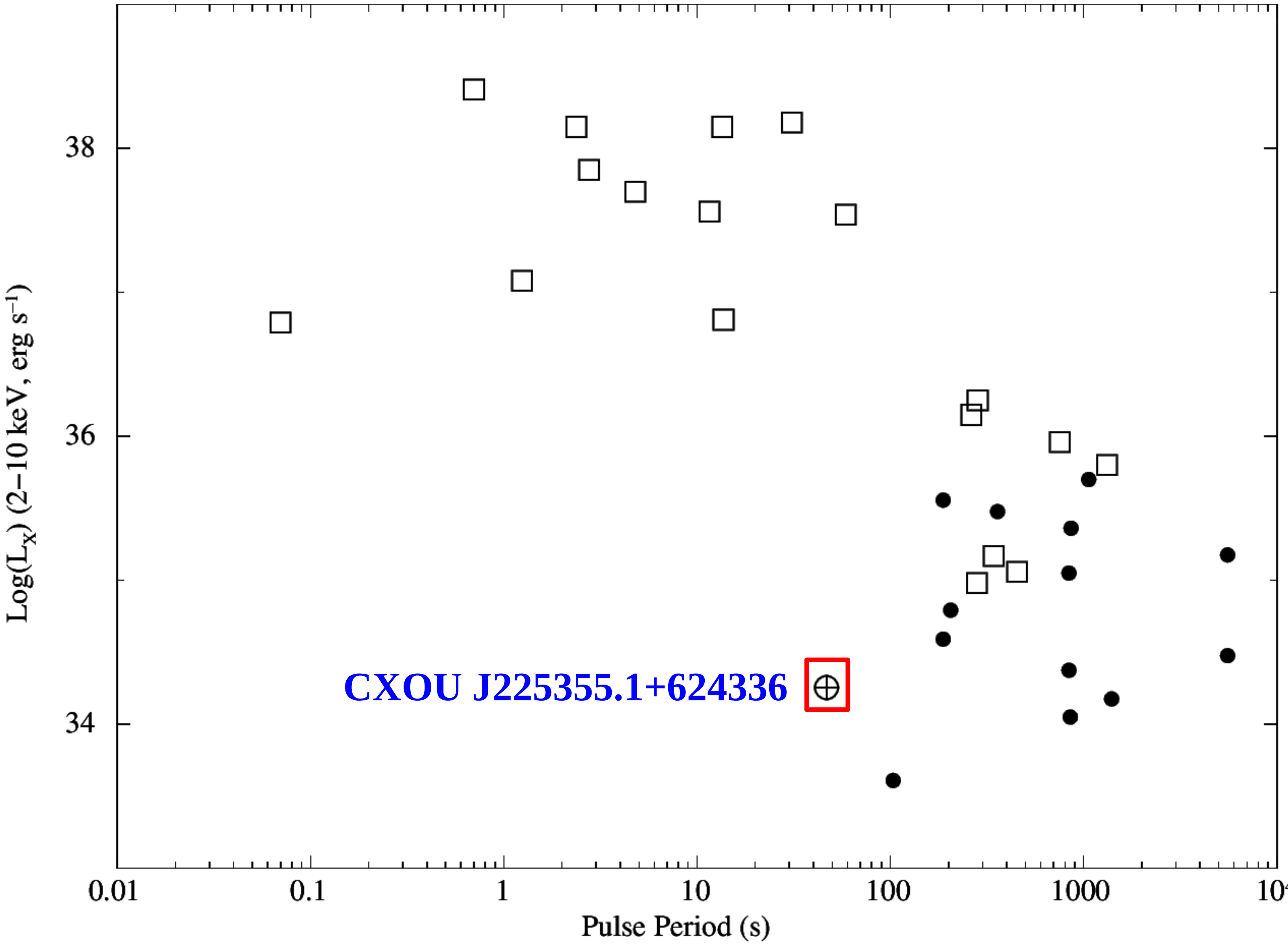

XMM-Newton observation of CXOU J225355

Analysis of an archival observation of ~30 ks,
performed on February 28th, 2014 (MJD 56716)
⇓
extension of the X-ray history
of the source to more than two decades

Results reported in La Palombara et al. 2021, A&A 649

Instrument	Filter	Mode	Time resolution	Net exposure time (ks)	Extraction radius (arcsec)	Net count rate (counts s^{-1})
pn	Thin 1	Full frame	73 ms	$\boxed{20.4}$	30	0.43 ± 0.03
MOS1	Thin 1	Full frame	2.7 s	$\boxed{25.1}$	30	0.134 ± 0.002
MOS2	Thin 1	Full frame	2.7 s	$\boxed{25.2}$	30	0.131 ± 0.002
RGS1	–	Spectroscopy	4.8 s	29.0	–	–
RGS2	–	Spectroscopy	9.6 s	29.0	–	–

⇓

EPIC net exposure time of 20-25 ks after removal of time intervals affected by SP flares

XMM-Newton observation of CXOU J225355: timing analysis

- P_{spin} = 46.753 ± 0.003 s
- Pulse profile with 3 peaks and energy dependence:
  - first and last peak more evident at low energies
  - middle peak more evident at high energies
- Flux variability almost constant with energy: PF = 40-45 %

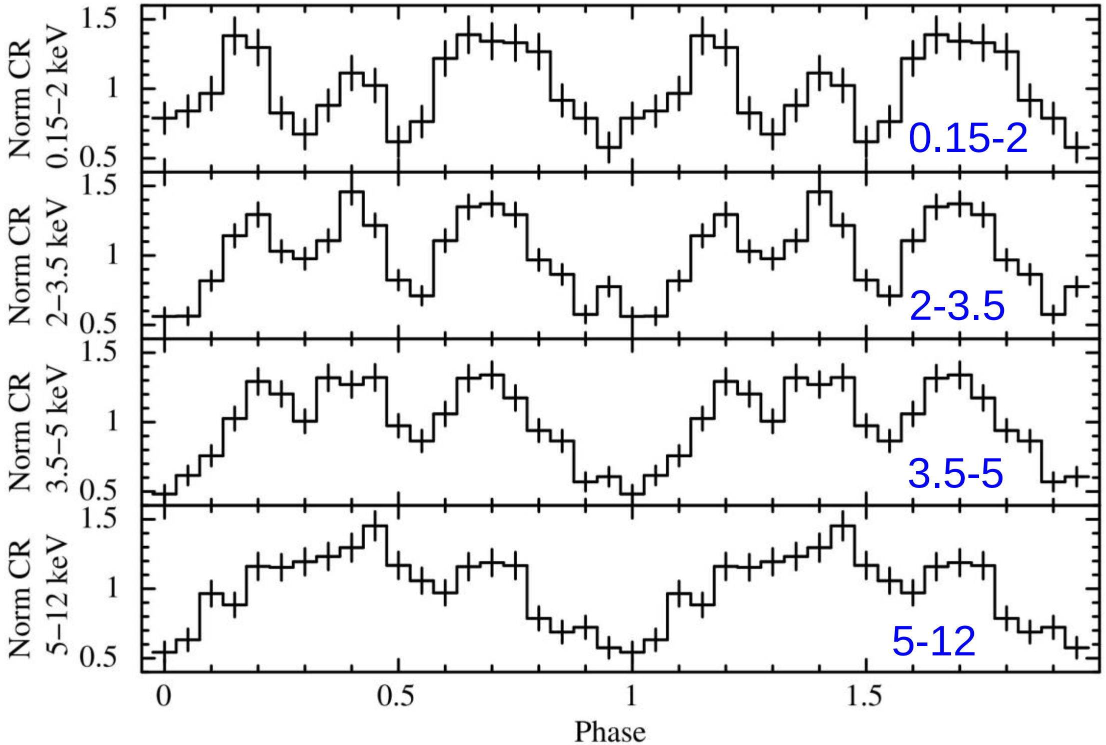

XMM-Newton observation of CXOU J225355: EPIC spectral analysis

EPIC time-averaged continuum spectra described with 4 different emission models:

1) 2 single-component non-thermal models

- absorbed power-law (PL) with a partial covering fraction absorption (TBPCF)
- absorbed cut-off power-law (CPL)

2) 2 double-component models with a PL + thermal component

- PL + blackbody (BB)
- PL + collisionally ionized gas (APEC)

XMM-Newton observation of CXOU J225355: EPIC spectral analysis

EPIC time-averaged continuum spectra described with 4 different emission models:

1) 2 single-component non-thermal models

- absorbed power-law (PL) with a partial covering fraction absorption (TBPCF)
- absorbed cut-off power-law (CPL)

2) 2 double-component models with a PL + thermal component

- PL + blackbody (BB)
- PL + collisionally ionized gas (APEC)

$\Downarrow$

1) all models provided an equally good fit
2) additional thermal component significant at 99 % c.l. in both the double-component models, with a neglibigle probability that it is spurious
3) weak positive residuals at E = 1.68 and 6.16 keV (and 0.98 keV for the CPL):

- features significant at 99 % c.l. when described with a Gaussian model
- Monte-Carlo simulations (SIMFTEST) $\Rightarrow$ high probability that these features are spurious

XMM-Newton observation of CXOU J225355: EPIC spectral analysis

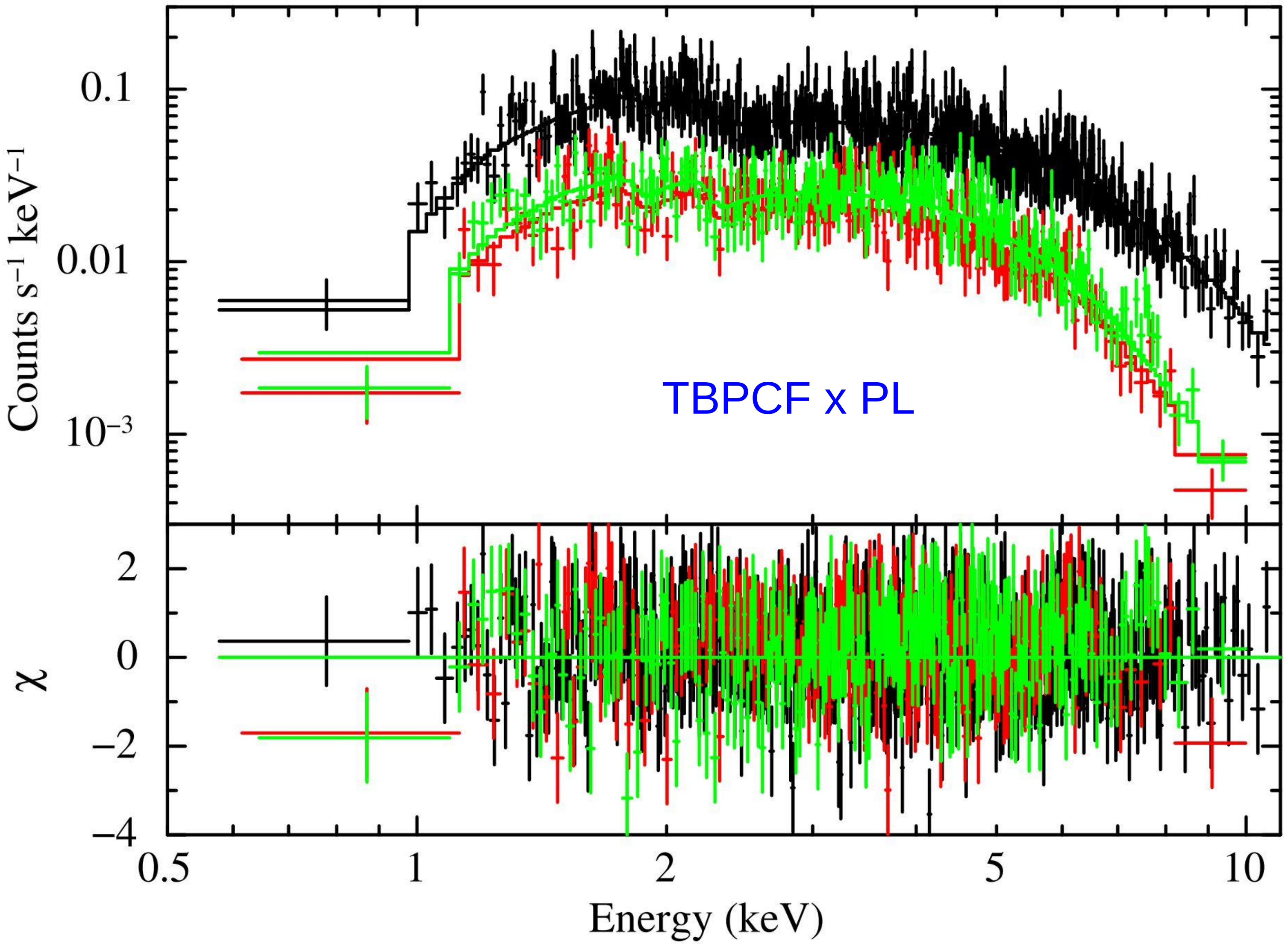

XMM-Newton observation of CXOU J225355: EPIC spectral analysis

Model parameter	– Unit	TBPCF×PL value	CPL value	PL+BB value	PL+APEC value
TBABS N_H	$\times 10^{22}$ cm^{-2}	$2.0^{+0.3}_{-0.2}$	1.6 ± 0.2	4.1 ± 0.4	$4.0^{+0.3}_{-0.4}$
TBPCF N_H	$\times 10^{22}$ cm^{-2}	$6.7^{+2.1}_{-1.7}$	–	–	–
TBPCF covering fraction	–	$0.63^{+0.07}_{-0.08}$	–	–	–
Γ	–	$1.66^{+0.14}_{-0.13}$	0 ± 0.3	$1.50^{+0.09}_{-0.08}$	1.49 ± 0.08
E_{cut}	keV	–	$4.0^{+1.1}_{-0.8}$	–	–
$Flux_{CPL/PL}$ (0.5–10 keV) [a]	$\times 10^{-12}$ erg cm^{-2} s^{-1}	$6.4^{+0.9}_{-0.6}$	$3.88^{+0.16}_{-0.15}$	$5.5^{+0.4}_{-0.3}$	5.5 ± 0.3
$kT_{BB\ or\ APEC}$	eV	–	–	120 ± 10	140^{+30}_{-20}
$R_{BB}^{(b)}$	km	–	–	100^{+80}_{-50}	–
N_{APEC}	cm^{-5}	–	–	–	$0.6^{+1.2}_{-0.4}$
$Flux_{BB\ or\ APEC}$ (0.5–10 keV) [a]	$\times 10^{-11}$ erg cm^{-2} s^{-1}	–	–	$2.9^{+3.0}_{-1.5}$	22^{+21}_{-14}
$Flux_{BB\ or\ APEC}/Flux_{TOT}$ (0.5–10 keV)	–	–	–	84.0 %	97.6 %
$Flux_{BB\ or\ APEC}/Flux_{TOT}$ (0.01–100 keV)	–	–	–	78.5 %	99.6 %
Unabsorbed flux (0.5–10 keV)	$\times 10^{-11}$ erg cm^{-2} s^{-1}	$0.64^{+0.09}_{-0.06}$	$0.39^{+0.01}_{-0.02}$	$3.4^{+3.0}_{-1.5}$	23^{+20}_{-14}
Luminosity (0.5–10 keV) [b]	$\times 10^{34}$ erg s^{-1}	$1.8^{+0.3}_{-0.2}$	1.10 ± 0.04	10^{+8}_{-5}	60^{+60}_{-40}
χ^2_ν/d.o.f.	–	0.95/920	0.96/921	0.95/920	0.96/920

[a] Corrected for absorption. [b] Assuming a source distance of $d = 5$ kpc.

$\Downarrow$

equally good fit with all models

XMM-Newton observation of CXOU J225355: EPIC spectral analysis

Model parameter	– Unit	TBPCF×PL value	CPL value	PL+BB value	PL+APEC value
TBABS N_H	$\times10^{22}$ cm^{-2}	$2.0^{+0.3}_{-0.2}$	1.6 ± 0.2	4.1 ± 0.4	$4.0^{+0.3}_{-0.4}$
TBPCF N_H	$\times10^{22}$ cm^{-2}	$6.7^{+2.1}_{-1.7}$	–	–	–
TBPCF covering fraction	–	$0.63^{+0.07}_{-0.08}$	–	–	–
Γ	–	$1.66^{+0.14}_{-0.13}$	0 ± 0.3	$1.50^{+0.09}_{-0.08}$	1.49 ± 0.08
E_{cut}	keV	–	$4.0^{+1.1}_{-0.8}$	–	–
Flux$_{CPL/PL}$ (0.5–10 keV) [a]	$\times10^{-12}$ erg cm^{-2} s^{-1}	$6.4^{+0.9}_{-0.6}$	$3.88^{+0.16}_{-0.15}$	$5.5^{+0.4}_{-0.3}$	5.5 ± 0.3
$kT_{BB\ or\ APEC}$	eV	–	–	120 ± 10	140^{+30}_{-20}
$R_{BB}^{(b)}$	km	–	–	100^{+80}_{-50}	–
N_{APEC}	cm^{-5}	–	–	–	$0.6^{+1.2}_{-0.4}$
Flux$_{BB\ or\ APEC}$ (0.5–10 keV) [a]	$\times10^{-11}$ erg cm^{-2} s^{-1}	–	–	$2.9^{+3.0}_{-1.5}$	22^{+21}_{-14}
Flux$_{BB\ or\ APEC}$/Flux$_{TOT}$ (0.5–10 keV)	–	–	–	84.0 %	97.6 %
Flux$_{BB\ or\ APEC}$/Flux$_{TOT}$ (0.01–100 keV)	–	–	–	78.5 %	99.6 %
Unabsorbed flux (0.5–10 keV)	$\times10^{-11}$ erg cm^{-2} s^{-1}	$0.64^{+0.09}_{-0.06}$	$0.39^{+0.01}_{-0.02}$	$3.4^{+3.0}_{-1.5}$	23^{+20}_{-14}
Luminosity (0.5–10 keV) [b]	$\times10^{34}$ erg s^{-1}	$1.8^{+0.3}_{-0.2}$	1.10 ± 0.04	10^{+8}_{-5}	60^{+60}_{-40}
χ^2_ν/d.o.f.	–	0.95/920	0.96/921	0.95/920	0.96/920

[a] Corrected for absorption. [b] Assuming a source distance of $d = 5$ kpc.

$\Downarrow$

rather high absorption: $N_H \sim (2\text{-}4) \times 10^{22}$ cm^{-2}

XMM-Newton observation of CXOU J225355: EPIC spectral analysis

Model parameter	– Unit	TBPCF×PL value	CPL value	PL+BB value	PL+APEC value
TBABS N_H	$\times 10^{22}$ cm^{-2}	$2.0^{+0.3}_{-0.2}$	1.6 ± 0.2	4.1 ± 0.4	$4.0^{+0.3}_{-0.4}$
TBPCF N_H	$\times 10^{22}$ cm^{-2}	$6.7^{+2.1}_{-1.7}$	–	–	–
TBPCF covering fraction	–	$0.63^{+0.07}_{-0.08}$	–	–	–
Γ	–	$1.66^{+0.14}_{-0.13}$	0 ± 0.3	$1.50^{+0.09}_{-0.08}$	1.49 ± 0.08
E_{cut}	keV	–	$4.0^{+1.1}_{-0.8}$	–	–
$\mathrm{Flux}_{CPL/PL}$ (0.5–10 keV) [a]	$\times 10^{-12}$ erg cm^{-2} s^{-1}	$6.4^{+0.9}_{-0.6}$	$3.88^{+0.16}_{-0.15}$	$5.5^{+0.4}_{-0.3}$	5.5 ± 0.3
$kT_{\mathrm{BB\ or\ APEC}}$	eV	–	–	120 ± 10	140^{+30}_{-20}
$R_{BB}^{(b)}$	km	–	–	100^{+80}_{-50}	–
N_{APEC}	cm^{-5}	–	–	–	$0.6^{+1.2}_{-0.4}$
$\mathrm{Flux}_{\mathrm{BB\ or\ APEC}}$ (0.5–10 keV) [a]	$\times 10^{-11}$ erg cm^{-2} s^{-1}	–	–	$2.9^{+3.0}_{-1.5}$	22^{+21}_{-14}
$\mathrm{Flux}_{\mathrm{BB\ or\ APEC}}/\mathrm{Flux}_{TOT}$ (0.5–10 keV)	–	–	–	84.0 %	97.6 %
$\mathrm{Flux}_{\mathrm{BB\ or\ APEC}}/\mathrm{Flux}_{TOT}$ (0.01–100 keV)	–	–	–	78.5 %	99.6 %
Unabsorbed flux (0.5–10 keV)	$\times 10^{-11}$ erg cm^{-2} s^{-1}	$0.64^{+0.09}_{-0.06}$	$0.39^{+0.01}_{-0.02}$	$3.4^{+3.0}_{-1.5}$	23^{+20}_{-14}
Luminosity (0.5–10 keV) [b]	$\times 10^{34}$ erg s^{-1}	$1.8^{+0.3}_{-0.2}$	1.10 ± 0.04	10^{+8}_{-5}	60^{+60}_{-40}
χ^2_ν/d.o.f.	–	0.95/920	0.96/921	0.95/920	0.96/920

[a] Corrected for absorption. [b] Assuming a source distance of $d = 5$ kpc.

$\Downarrow$

rather hard spectrum: $\Gamma \sim 0 - 1.5$

XMM-Newton observation of CXOU J225355: EPIC spectral analysis

Model parameter	– Unit	TBPCF×PL value	CPL value	PL+BB value	PL+APEC value
TBABS N_H	$\times 10^{22}$ cm^{-2}	$2.0^{+0.3}_{-0.2}$	1.6 ± 0.2	4.1 ± 0.4	$4.0^{+0.3}_{-0.4}$
TBPCF N_H	$\times 10^{22}$ cm^{-2}	$6.7^{+2.1}_{-1.7}$	–	–	–
TBPCF covering fraction	–	$0.63^{+0.07}_{-0.08}$	–	–	–
Γ	–	$1.66^{+0.14}_{-0.13}$	0 ± 0.3	$1.50^{+0.09}_{-0.08}$	1.49 ± 0.08
E_{cut}	keV	–	$4.0^{+1.1}_{-0.8}$	–	–
$\text{Flux}_{\text{CPL/PL}}$ (0.5–10 keV) [a]	$\times 10^{-12}$ erg cm^{-2} s^{-1}	$6.4^{+0.9}_{-0.6}$	$3.88^{+0.16}_{-0.15}$	$5.5^{+0.4}_{-0.3}$	5.5 ± 0.3
$kT_{\text{BB or APEC}}$	eV	–	–	120 ± 10	140^{+30}_{-20}
$R^{(b)}_{BB}$	km	–	–	100^{+80}_{-50}	–
N_{APEC}	cm^{-5}	–	–	–	$0.6^{+1.2}_{-0.4}$
$\text{Flux}_{\text{BB or APEC}}$ (0.5–10 keV) [a]	$\times 10^{-11}$ erg cm^{-2} s^{-1}	–	–	$2.9^{+3.0}_{-1.5}$	22^{+21}_{-14}
$\text{Flux}_{\text{BB or APEC}}/\text{Flux}_{\text{TOT}}$ (0.5–10 keV)	–	–	–	84.0 %	97.6 %
$\text{Flux}_{\text{BB or APEC}}/\text{Flux}_{\text{TOT}}$ (0.01–100 keV)	–	–	–	78.5 %	99.6 %
Unabsorbed flux (0.5–10 keV)	$\times 10^{-11}$ erg cm^{-2} s^{-1}	$0.64^{+0.09}_{-0.06}$	$0.39^{+0.01}_{-0.02}$	$3.4^{+3.0}_{-1.5}$	23^{+20}_{-14}
Luminosity (0.5–10 keV) [b]	$\times 10^{34}$ erg s^{-1}	$1.8^{+0.3}_{-0.2}$	1.10 ± 0.04	10^{+8}_{-5}	60^{+60}_{-40}
χ^2_ν/d.o.f.	–	0.95/920	0.96/921	0.95/920	0.96/920

[a] Corrected for absorption. [b] Assuming a source distance of $d = 5$ kpc.

$\Downarrow$

Flux of the non-thermal component ~ (4-6) x 10^{-12} erg cm^{-2} s^{-1}

XMM-Newton observation of CXOU J225355: EPIC spectral analysis

Model parameter	– Unit	TBPCF×PL value	CPL value	PL+BB value	PL+APEC value
TBABS N_H	$\times10^{22}$ cm^{-2}	$2.0^{+0.3}_{-0.2}$	1.6 ± 0.2	4.1 ± 0.4	$4.0^{+0.3}_{-0.4}$
TBPCF N_H	$\times10^{22}$ cm^{-2}	$6.7^{+2.1}_{-1.7}$	–	–	–
TBPCF covering fraction	–	$0.63^{+0.07}_{-0.08}$	–	–	–
Γ	–	$1.66^{+0.14}_{-0.13}$	0 ± 0.3	$1.50^{+0.09}_{-0.08}$	1.49 ± 0.08
E_{cut}	keV	–	$4.0^{+1.1}_{-0.8}$	–	–
Flux$_{CPL/PL}$ (0.5–10 keV) $^{(a)}$	$\times10^{-12}$ erg cm^{-2} s^{-1}	$6.4^{+0.9}_{-0.6}$	$3.88^{+0.16}_{-0.15}$	$5.5^{+0.4}_{-0.3}$	5.5 ± 0.3
$kT_{BB\ or\ APEC}$	eV	–	–	120 ± 10	140^{+30}_{-20}
$R_{BB}^{(b)}$	km	–	–	100^{+80}_{-50}	–
N_{APEC}	cm^{-5}	–	–	–	$0.6^{+1.2}_{-0.4}$
Flux$_{BB\ or\ APEC}$ (0.5–10 keV) $^{(a)}$	$\times10^{-11}$ erg cm^{-2} s^{-1}	–	–	$2.9^{+3.0}_{-1.5}$	22^{+21}_{-14}
Flux$_{BB\ or\ APEC}$/Flux$_{TOT}$ (0.5–10 keV)	–	–	–	84.0 %	97.6 %
Flux$_{BB\ or\ APEC}$/Flux$_{TOT}$ (0.01–100 keV)	–	–	–	78.5 %	99.6 %
Unabsorbed flux (0.5–10 keV)	$\times10^{-11}$ erg cm^{-2} s^{-1}	$0.64^{+0.09}_{-0.06}$	$0.39^{+0.01}_{-0.02}$	$3.4^{+3.0}_{-1.5}$	23^{+20}_{-14}
Luminosity (0.5–10 keV) $^{(b)}$	$\times10^{34}$ erg s^{-1}	$1.8^{+0.3}_{-0.2}$	1.10 ± 0.04	10^{+8}_{-5}	60^{+60}_{-40}
χ^2_ν/d.o.f.	–	0.95/920	0.96/921	0.95/920	0.96/920

$^{(a)}$Corrected for absorption. $^{(b)}$Assuming a source distance of $d = 5$ kpc.

$\Downarrow$

Flux of the thermal component ~ 10-100 times higher: overestimated due to the combination of high absorption and low temperature?

Phase-resolved spectral analysis - 1

Independent fit of the two spectra:

- f_x decreases of ~ 20 % from A to B
- Both BB and APEC components significant at 99 % c.l.
- Consistent values of almost all parameters (only N_H decreases for PL+BB/APEC model)
- f_x reduction of ~ 20 % for PL and ~ 60-70 % for BB/APEC, but with large uncertainties

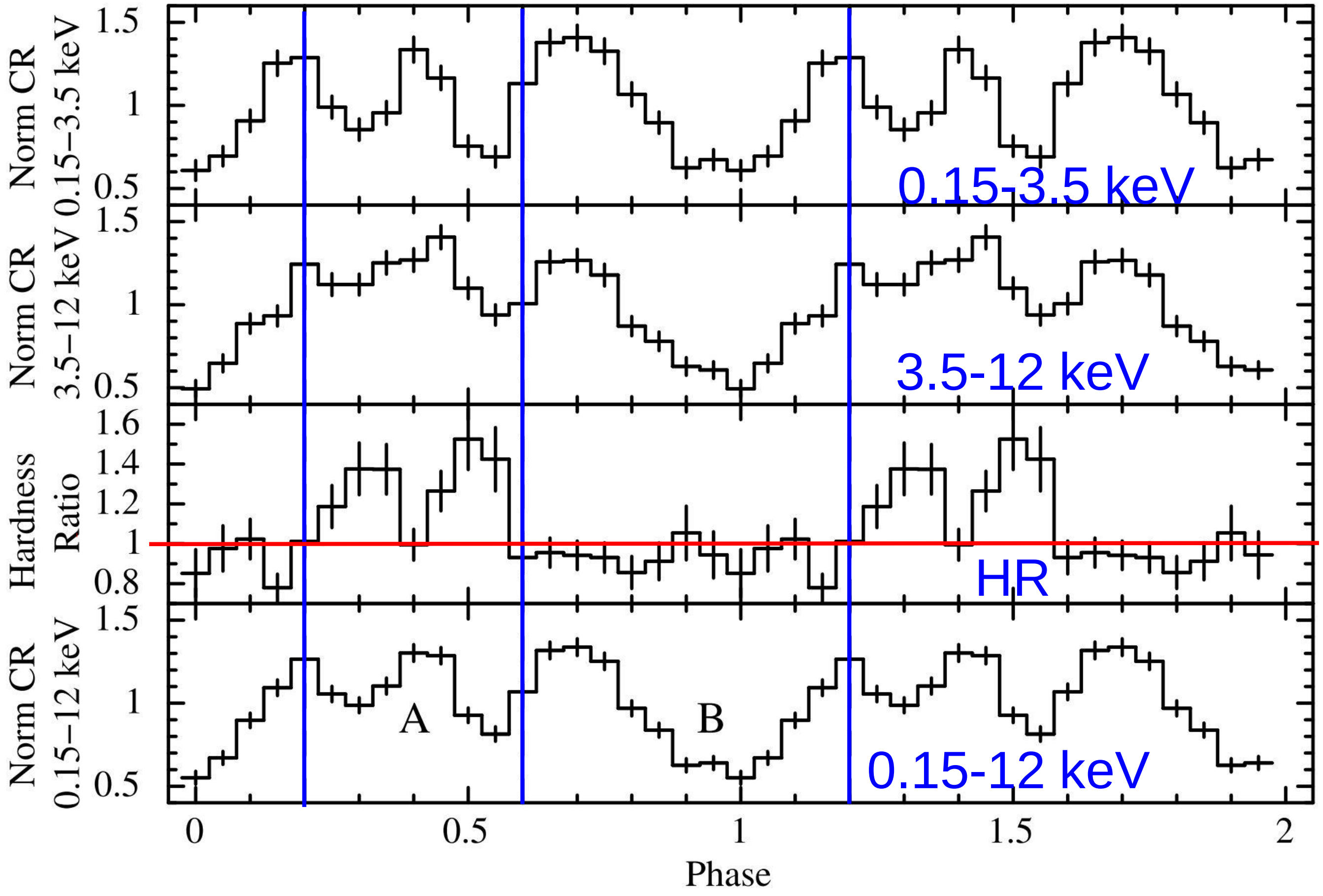

⇒

- no clear evidence of a spectral variation
- possible variation in the relative contribution of the two components for the PL+BB/APEC models

Phase-resolved spectral analysis - 2

Simultaneous fit of phase-resolved spectra:

1) Single non-thermal component models:

- only normalization variation (common N_H and Γ) rejected by the data
  $\Rightarrow$ also a variation of N_H, Γ or E_{cut} is necessary
- constant CPL component rejected by the data
- constant PL component possible only with a large variation of TBPCF parameters

2) Two-component models:

Data consistent with a variation of only the relative contribution of the two components, but:

- in all cases, data inconsistent with a constant PL component
- constant thermal component:
  - rejected if only PL normalization varies
  - possible if either N_H or Γ vary

$\Downarrow$

data consistent with a constant thermal component

Phase-resolved spectral analysis - 3

Spectrum A: emission feature at E ~ 6.1 keV

Gaussian component significant at 99 % c.l., with E = 6.12±0.08 keV, σ = 80(+110/-80) eV, EW = 130(+90/-80) eV

⇓

inconsistent with neutral Fe emission line

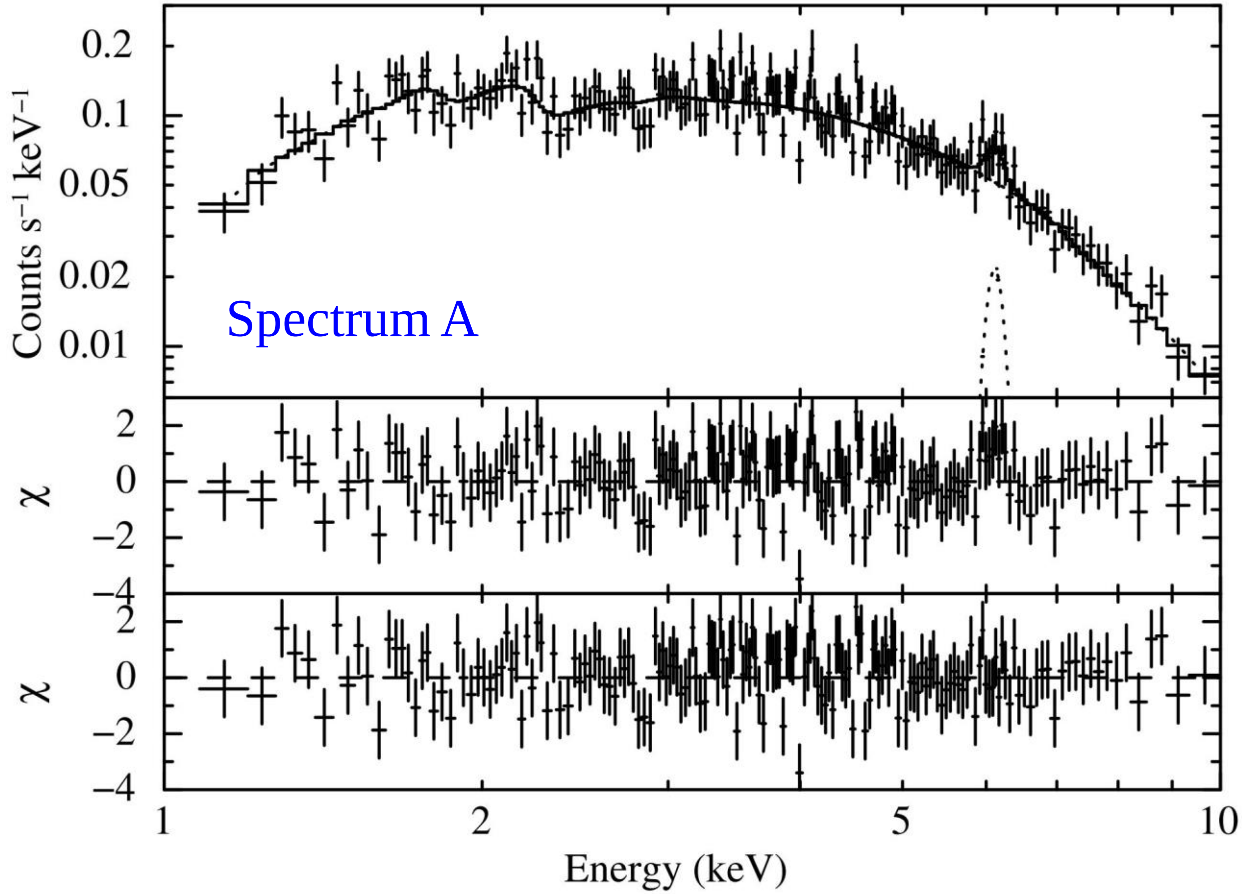

- Weak statistical improvement in the spectral fit ($\Delta\chi_\nu^2$ = 0.05)
- SIMFTEST ⇒ < 1 % probability of being a spurious component

⇒ ?

Flux long-term evolution

- Flux rather stable (variations of ± 30 % at most)
- d = 5 kpc ⇒ $L_X < 10^{36}$ erg s^{-1}

⇓

- reduced variability
- relatively low luminosity

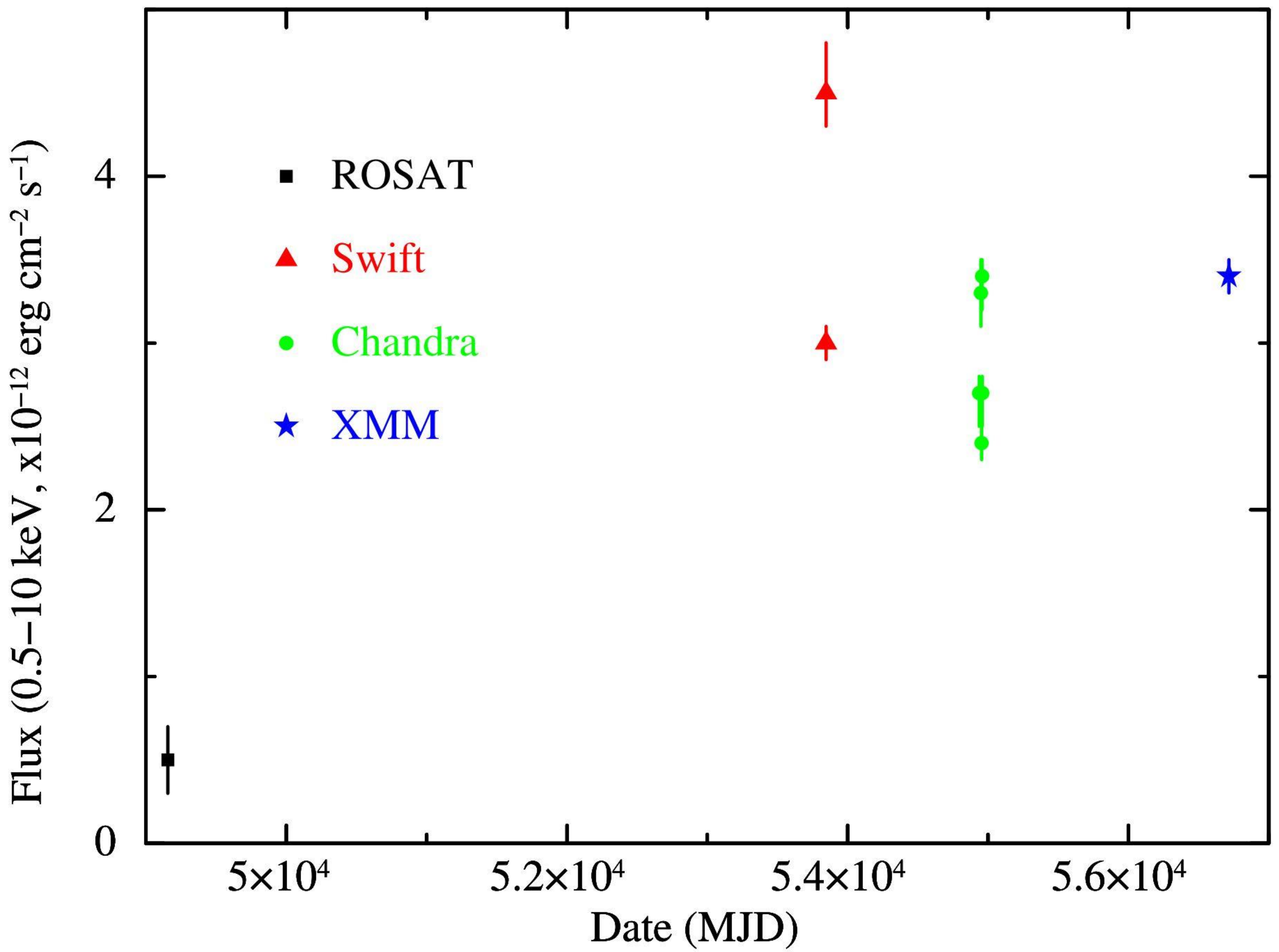

Spin period long-term evolution

$P_{spin,2014}$ = 46.753(3) s

P_{spin} increase much larger than the systematic error of 0.02 s, assumed based on the uncertainties due to the NS orbit

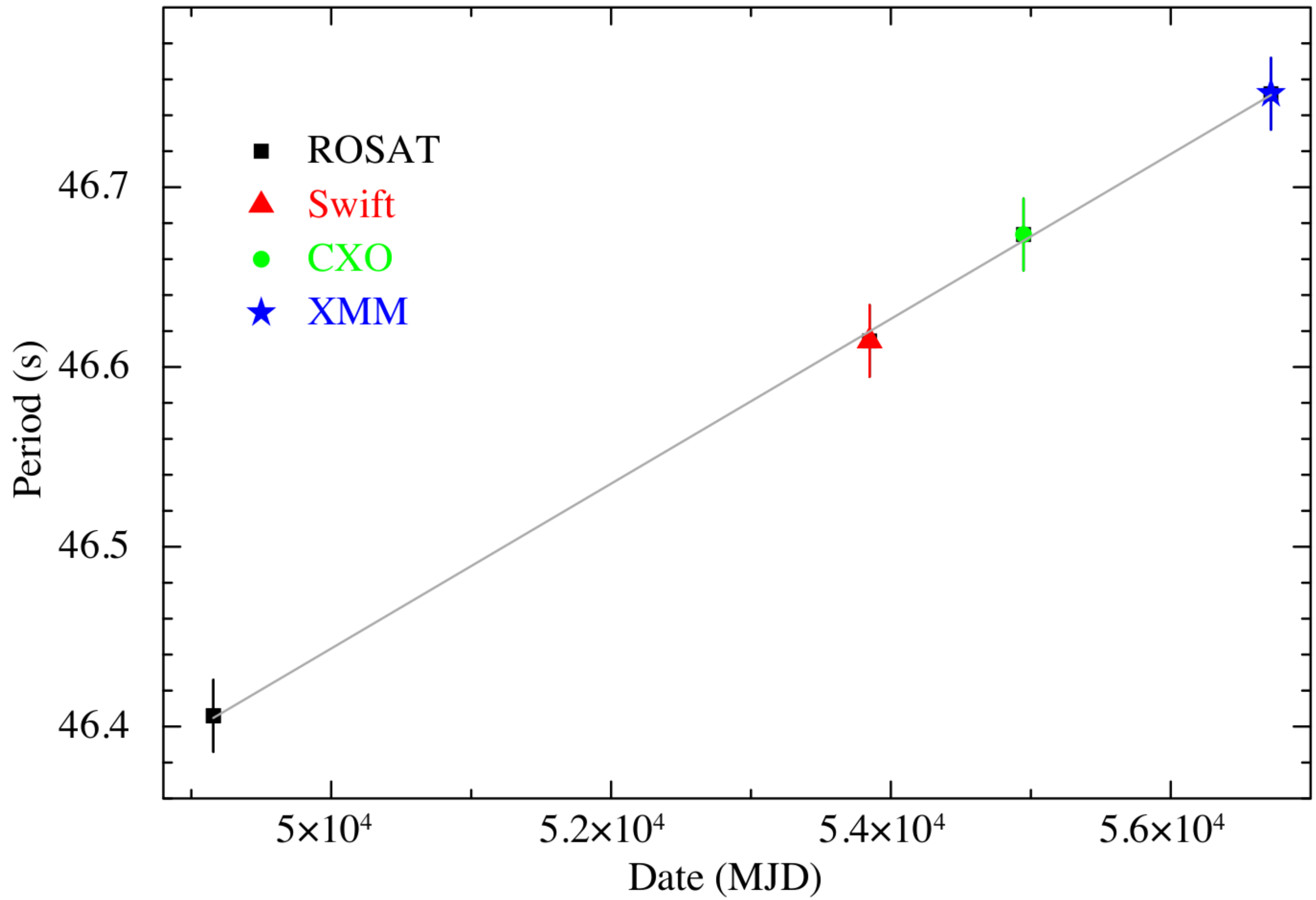

$P_{spin,2014}$ fully consistent with a constant pulsar spin down at an average $\dot{P}$ = 5.3 x 10^{-10} s s^{-1}, in agreement with Esposito et al. (2013)

Timing and spectral properties - 1

Comparison with previous *Chandra* and *Swift* results:

- Confirmation of the three-peak pulse profile
- Discovery of the spectral variability along the spin phase
- Very similar absorption (N_H = 2 x 10^{22} cm^{-2}) for the two models with only a non-thermal component (CPL and partially-covered PL)

Estimated Galactic value in the source direction: $N_{H,\ Gal}$ = 9 x 10^{21} cm^{-2}

⇓

≥ 50 % of the total absorption is due to a local component

⇓

inhomogeneous absorber medium in the case of the partially-covered PL model, which can be reasonably ascribed to the Be, clumpy, polar wind crossing the line of sight to the X-ray source

Timing and spectral properties - 2

1) Possible additional thermal component:

- Common spectral feature in several BeXBs (either persistent with low luminosity or transient with high luminosity)
- Low estimated temperature (kT = 120-140 eV) compared with BeXBs of similar luminosity
- Estimated unabsorbed flux of this component largely dominates the total source flux
- Size of the thermal emission region significantly larger than the NS size

$\Downarrow$

we disfavour the presence of such a thermal component

2) Spectral variability with the pulse phase proved with the phase-resolved spectral analysis

Conclusions

XMM-Newton results confirm that CXOU J225355.1+624336 is characterised by:

- Low luminosity: $L_X = 10^{34\text{-}35}$ erg s^{-1}
- Limited variability: f_X variations within ± 30 %
- P_{spin} consistent with a constant pulsar spin down

$\Downarrow$

wind-accretion scenario of the pulsating NS from the companion Be star

Source classification:

- Additional evidence of the similarity between CXOU J225355.1+624336 and X Per-like sources
- P_{spin} = 46.753 s $\Rightarrow$ source with the shortest pulse period in the class of persistent BeXBs

Future perspectives

Spectral investigation of the poorly studied HMXB **4U 0728-25**:

- Optical counterpart: O8-9 Ve type star (Negueruela et al. 1996)
- Estimated distance: d = 7.6±0.9 kpc (based on Gaia EDR3 data)
- P_{spin} = 103.2±0.1 s, $P_{orb} \cong$ 34.5 days (Corbet & Peele 1997)
- Almost steady emission with no brightening, based on source monitoring performed with *Swift* BAT between 2005 and 2016 (Corbet et al. 2016)
- Included in the catalogues of persistent X-ray sources detected with *BeppoSAX* WFC (Capitanio et al. 2011) and INTEGRAL IBIS (Bird et al. 2016)
- $f_X \sim$ a few 10^{-11} erg cm^{-2} s^{-1} $\Rightarrow$ $L_X \sim$ a few 10^{35} erg s^{-1}

$\Downarrow$

strong candidate as X-Persei–like persistent BeXB

Future perspectives

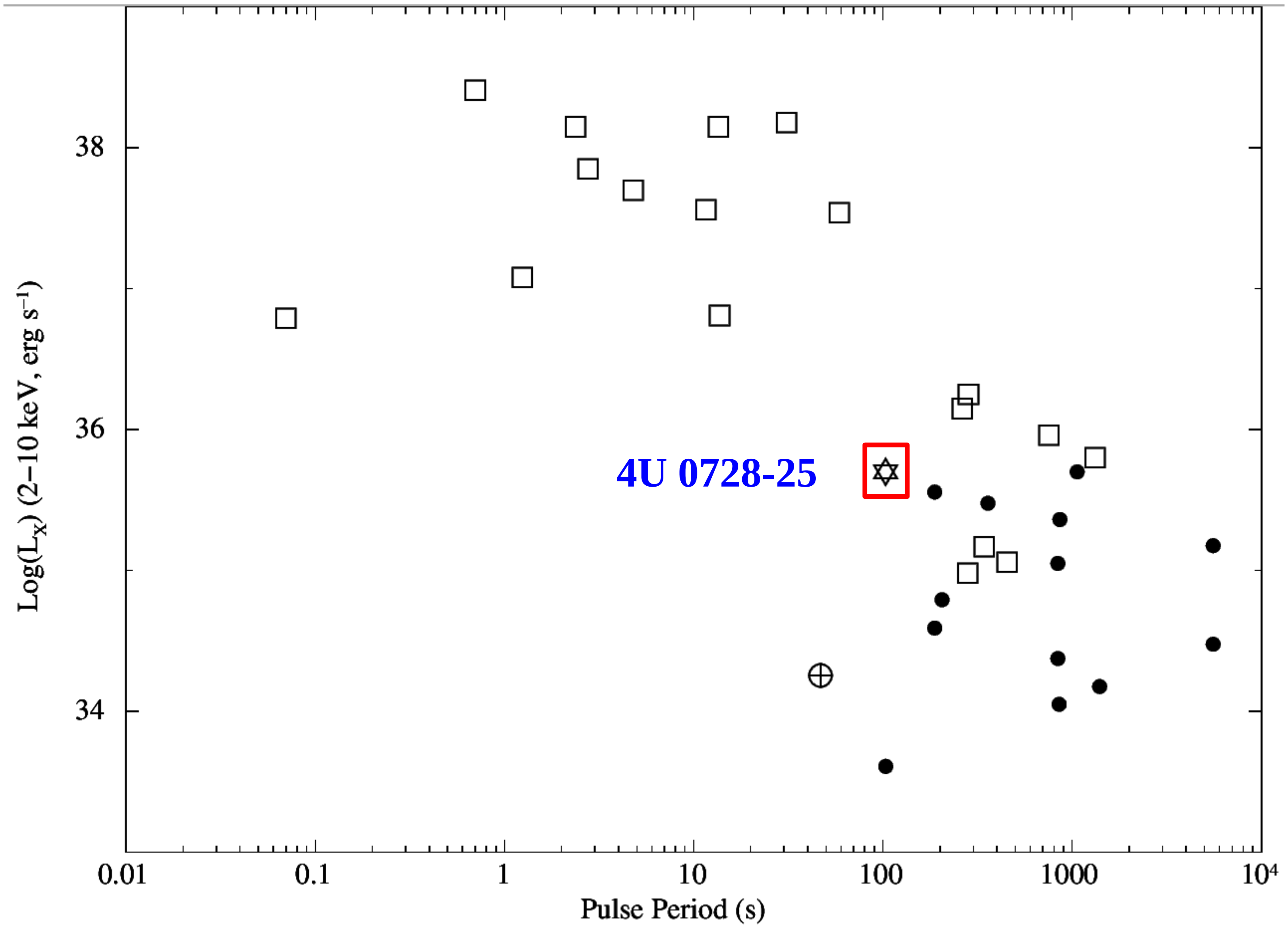

Future perspectives

Spectral investigation of the poorly studied HMXB **4U 0728-25**:

- Optical counterpart: O8-9 Ve type star (Negueruela et al. 1996)
- Estimated distance: d = 7.6±0.9 kpc (based on Gaia EDR3 data)
- P_{spin} = 103.2±0.1 s, $P_{orb} \cong$ 34.5 days (Corbet & Peele 1997)
- Almost steady emission with no brightening, based on source monitoring performed with *Swift* BAT between 2005 and 2016 (Corbet et al. 2016)
- Included in the catalogues of persistent X-ray sources detected with *BeppoSAX* WFC (Capitanio et al. 2011) and INTEGRAL IBIS (Bird et al. 2016)
- $f_X \sim$ a few 10^{-11} erg cm^{-2} s^{-1} $\Rightarrow$ $L_X \sim$ a few 10^{35} erg s^{-1}

$\Downarrow$

strong candidate as X-Persei–like persistent BeXB

Observation proposal accepted in Priority C for the *XMM-Newton* AO21

$\Downarrow$

STAY TUNED!

Backup slides

Single-component model

Parameter	Spectrum A	Spectrum B
TBPCF×PL		
TBABS N_H ($\times10^{22}$ cm^{-2})	$1.9^{+0.6}_{-0.9}$	$1.8^{+0.3}_{-0.4}$
TBPCF N_H ($\times10^{22}$ cm^{-2})	6 ± 2	6 ± 2
TBPCF covering fraction	$0.7^{+0.2}_{-0.1}$	0.6 ± 0.1
Γ	1.5 ± 0.2	$1.6^{+0.2}_{-0.1}$
Flux$_{PL}$ (0.5–10 keV) [a]	$6.7^{+1.1}_{-0.8}$	$5.4^{+1.0}_{-0.6}$
Luminosity (0.5–10 keV) [b]	$1.9^{+0.3}_{-0.2}$	$1.5^{+0.3}_{-0.1}$
χ^2_ν/d.o.f.	1.12/176	1.01/225
CPL		
TBABS N_H ($\times10^{22}$ cm^{-2})	$1.8^{+0.5}_{-0.4}$	$1.5^{+0.2}_{-0.3}$
Γ	-0.2 ± 0.5	$0.2^{+0.3}_{-0.4}$
E_{cut} (keV)	4^{+2}_{-1}	4^{+2}_{-1}
Flux$_{CPL}$ (0.5–10 keV) [a]	$4.3^{+0.3}_{-0.2}$	3.5 ± 0.2
Luminosity (0.5–10 keV) [b]	1.23 ± 0.08	$0.99^{+0.06}_{-0.05}$
χ^2_ν/d.o.f.	1.15/177	1.02/226

Notes. [a]Corrected for absorption, $\times10^{-12}$ erg cm^{-2} s^{-1}. [b]$\times10^{34}$ erg s^{-1}, assuming a source distance of $d = 5$ kpc. [c]Assuming a source distance of $d = 5$ kpc.

Double-component model

Parameter	Spectrum A	Spectrum B
PL+BB		
TBABS N_H ($\times10^{22}$ cm^{-2})	$4.6^{+0.8}_{-0.7}$	3.5 ± 0.5
Γ	1.4 ± 0.1	1.5 ± 0.1
Flux$_{PL}$ (0.5–10 keV) [a]	6.2 ± 0.5	$4.8^{+0.4}_{-0.3}$
kT_{BB} (eV)	120 ± 20	120^{+10}_{-20}
R_{BB} (km) [c]	110^{+150}_{-70}	80^{+90}_{-50}
Flux$_{BB}$ (0.5–10 keV) [a]	40^{+90}_{-30}	20^{+20}_{-10}
Flux$_{BB}$/Flux$_{TOT}$ (0.5–10 keV)	85.8%	77.0%
Flux$_{BB}$/Flux$_{TOT}$ (0.01–100 keV)	76.9%	70.7%
Unabsorbed flux (0.5–10 keV) [a]	50^{+90}_{-30}	20^{+30}_{-10}
Luminosity (0.5–10 keV) [b]	14^{+25}_{-9}	6^{+7}_{-3}
χ^2_ν/d.o.f.	1.11/176	1.01/225
PL+APEC		
TBABS N_H ($\times10^{22}$ cm^{-2})	4.4 ± 0.7	$3.4^{+0.4}_{-0.5}$
Γ	$1.4^{+0.1}_{-0.2}$	1.5 ± 0.1
Flux$_{PL}$ (0.5–10 keV) [a]	$6.0^{+0.6}_{-0.4}$	4.8 ± 0.3
kT_{APEC} (eV)	140^{+40}_{-30}	140^{+40}_{-20}
N_{APEC} (cm^{-5})	$1.0^{+0.7}_{-0.8}$	$0.30^{+0.23}_{-0.25}$
Flux$_{APEC}$ (0.5–10 keV) [a]	300^{+900}_{-200}	120^{+210}_{-90}
Flux$_{APEC}$/Flux$_{TOT}$ (0.5–10 keV)	98.2%	95.9%
Flux$_{APEC}$/Flux$_{TOT}$ (0.01–100 keV)	99.6%	99.3%
Unabsorbed flux (0.5–10 keV) [a]	300^{+1000}_{-200}	120^{+210}_{-90}
Luminosity (0.5–10 keV) [b]	100^{+290}_{-70}	30^{+60}_{-20}
χ^2_ν/d.o.f.	1.11/176	1.02/225

Notes. [a]Corrected for absorption, $\times10^{-12}$ erg cm^{-2} s^{-1}. [b]$\times10^{34}$ erg s^{-1}, assuming a source distance of $d = 5$ kpc. [c]Assuming a source distance of $d = 5$ kpc.